

Performance analysis and optimisation of the chiller-air handling units system with a wide range of ambient temperature

Nur I. Zulkafli^{a,*}, Mohamad F. Sukri^a, Musthafah Mohd Tahir^a, Asjufri Muhajir^a, Dawid P. Hanak^{b,c}

^a Centre for Advanced Research on Energy, Faculty of Mechanical Engineering, Universiti Teknikal Malaysia Melaka, Durian Tunggal, Melaka, 76100, Malaysia

^b Energy and Sustainability, Canfield University, School of Water, Energy and Environment, Bedfordshire, MK43 0AL, United Kingdom

^c Net Zero Industry Innovation Centre, Teesside University, Middlesbrough, TS1 3BA, United Kingdom

ARTICLE INFO

Keywords:

Chiller
Air handling unit
Cooling tower
HVAC
Linear programming model
Coefficient of performance
Power consumption

ABSTRACT

The integrated optimisation modelling for the chiller-air handling units system is developed for increasing the efficiency and energy utilisation of system. A building management system in the chillers network controls the cooling load to achieve the specified desired set temperature of the cooling air within the building can be satisfied. Unfortunately, the desired set point temperature of the cooling air is a fixed value and does not vary with the dynamic change of cooling demand with different ambient temperatures. Therefore, the power consumption of the chillers and the building cooling requirement with a wide range of different ambient temperatures is properly modelled by optimising the performance of chillers, air handling units, cooling towers, and water pumps. The linear programming model for the system is established to model a real representation of the chiller-air handling unit system. The result shows that the optimal coefficient of performance is greater by about 7%–10% than the current chiller system. The optimal power consumption of the chiller system reduces to 3%. Overall, the optimal decision solutions could be used as the potential improvement strategy to control the desired set point values in the building management system for efficient chiller-AHU system.

1. Introduction

The capability of efficient energy utilisation in heating, ventilation, and air conditioning (HVAC) system should be the major focus in achieving effective cooling demands and indoor thermal comfort. Globally, the HVAC system is the primary energy end-use that is reportedly accounted for 36% of emissions of greenhouse gases and 40% of worldwide energy consumption (ASHRAE, 2019). One of the best solutions to reduce energy consumption is optimising the HVAC system operation to obtain optimal control solutions. The HVAC system is made up of chillers, air handling units (AHU), cooling towers, and water pumps. The energy consumption can be optimised by analyzing the process integration of different equipment to satisfy the building cooling demand. In addition, the building cooling demand varies according to weather conditions (Chen et al., 2022). However, in the current conventional control of the HVAC system, the variation of the cooling demand has not been considered. The desired set point for return air temperature for the building is a constant value and does not impact by

the variation of the cooling demand due to weather conditions. Two cooling effects from the current operation of the chiller-AHU system are insufficient cooling which could result in an uncomfortable atmosphere within the building and an excess cooling effect that would decrease the chillers' performance. The cause of this is that the building cooling demand is undetermined and cannot be quantified by the changes in ambient temperatures (Zulkafli et al., 2022). Therefore, this study develops optimisation modelling for the whole integrated chiller-AHU system to evaluate the optimum time-varying COP profile. The optimisation technique of a Linear Programming (LP) Model, which considers the cooling load, energy efficiency, and electricity bill can be regarded as an ideal operational approach for the chiller-AHU units system. After improving the operational decisions of the chiller-AHU system for the building, energy savings can be measured. The assessment of energy saving is regarded as the energy performance indicator to calculate the energy rating score to earn recognition from the governmental energy agencies.

The assessment of the coefficient of performance (COP) for the

* Corresponding author.

E-mail address: nurizyan@utem.edu.my (N.I. Zulkafli).

<https://doi.org/10.1016/j.clet.2023.100643>

Received 23 February 2023; Received in revised form 16 April 2023; Accepted 21 May 2023

Available online 22 May 2023

2666-7908/© 2023 The Authors. Published by Elsevier Ltd. This is an open access article under the CC BY-NC-ND license (<http://creativecommons.org/licenses/by-nc-nd/4.0/>).

chiller system will allow for monitoring the main operating performance. If insufficient cooling capacity generation happens with high power consumption, the COP of chillers decreases. The chiller should run at its highest COP to produce the appropriate cooling capacity with a minimum amount of power consumption (Thangavelu et al., 2017). The study by Ho et al. (Ho and Yu, 2021) revealed that the cooling load, chilled water flow rate, and chilled water return temperature significantly affected the value of COP of the particular chiller. COP is typically not constant throughout operational time due to variations of control techniques (Liu et al., 2017) and fluctuation in cooling load demands (Sala-Cardoso et al., 2020) that substantially influence the power consumption profile. The chiller's coefficient of performance (COP), which is frequently assumed to remain constant is inconsistent with the real situation, particularly given that the chiller operates most of the time at partial load. The modelling of cooling demands in the optimisation approach can optimise the performance of the chillers and minimise electricity by finding the possibility and the adaptability of the chiller system (Shao et al., 2019). The cooling demands of the building are difficult to estimate because of inaccurate design information and insufficient operational data to estimate system performance (Huang et al., 2018). The cooling demands are affected by different outside ambient temperatures and the occupancy in the building (Kumar et al., 2022). For instance, the study was performed to evaluate optimum energy saving and cost benefits for weather-based energy systems (Chen et al., 2022). Similarly, a performance assessment was performed for the all-air and water-air systems under changing climate. The cooling demand for all-air systems was higher than that for water-air systems by about 18% for different weather climates (Velashjerdi Farahani et al., 2022).

The chiller-AHU system problem refers to the necessity to control the operation of the chillers network according to the cooling load requirements (Liao et al., 2017). The optimisation-based approach should include integrated modelling for the chiller, cooling tower, and air handling units, as the whole system is interdependent to operate efficiently. However, AHU units have rarely been considered as a part of the optimisation problem of the energy management system (EMS) of the central chiller plant. Usually, AHUs are not fully integrated with the EMS of the chiller system, although it will determine the actual cooling demand of the building. If the integration of chiller-AHU system is done and the room temperature is properly maintained with varied ambient temperatures, the linear or mixed integer linear programming model can offer the system's ideal operation. By carefully balancing the operation of fans, pumps, and chillers, the reduced overall power consumption of the system is possible to attain (Zhang and Grossmann, 2016). In a recent study, a 6.2% overall reduction in power requirement and a 12.3% decrease in electricity costs can be realised compared to conventional control of HVAC systems (Wang et al., 2022a).

The current practice of manual control is not accurate to achieve high operational efficiency since the operation of the chiller-AHU system heavily depends on the cooling demand variation and the integration of the whole system. The building management system (BMS) is the conventional control of the HVAC system. The BMS is the control system for the automatic regulation and control of the HVAC system by maintaining a predefined set point. The function of BMS is to control the flow of energy by identifying parameters for improvement. However, a fixed value is being set for the return air set point temperature of the building and it is not changing according to different ambient temperatures (Charef, 2022). The review of the sustainability framework for buildings discovered that changing the set point temperature according to the weather condition has resulted in reduction of energy consumption by 30% and carbon dioxide emissions by 56%, respectively (Kumar et al., 2022). However, the exact set point temperature that varies according to weather conditions is unknown. Only fixed values are being set based on normal practice by the building owner (Merkert et al., 2015). An optimisation modelling needs to be done by accounting for the integrated process of each set of equipment and the effect of weather conditions to

investigate the optimal decision solution, performance, and energy consumption of the chiller-AHU system. Therefore, the controlled operating parameters in the BMS are proposed to follow the optimal solution values, such as the return air temperature and chiller temperature for different ambient temperatures.

The optimisation model for chillers-air handling unit systems under various ambient temperatures will be the major literature topic of this study. Table 1 displays the list of main contributions on the study of chiller-AHUs system that considers energy consumption, cooling load and demand, COP and weather conditions. From the list comparison in Table 1, two main points to highlight the research gaps of the proposed study can be emphasized. Firstly, the study of optimisation modelling of chiller-AHUs system with the effects of ambient temperatures has not yet been reported in the literatures because most of the studies did not include the modelling of AHUs system as a part of the optimisation problem for the integrated chiller system.

The second points of research gap is on the method of optimisation approaches. Meta-heuristic methods have been popular in literary works of optimisation problems to efficiently enhance solutions and lessen the computational cost. Examples of methods that are frequently utilised in solving chiller problems are genetic algorithms, neural networks, and particle swarm optimisation. However, the capability to find convergence is typically difficult to achieve from these techniques. The complex optimisation problems can be solved effectively by the use of mathematical formulation techniques to deliver computable decisions and to effectively handle complex optimisation problems. The linear programming (LP) model is one of the mathematical formulation techniques. The LP model is formulated based on theoretical equations of the optimisation problem to achieve towards minimising or maximizing the objective function. The well formulated and global optimality-guaranteed model are the major benefits of the LP model to achieve quick and optimal solutions (Gbadamosi and Nwulu, 2021). The global optimal solution from the formulations of the LP model will be the baseline to investigate the current performance of the chiller-AHUs system.

In addition, none of these study presented detailed optimisation-based approach for chiller-AHUs system considering major operational aspects (e.g., energy consumption, cooling load, COP, sensible and latent heat) under a wide range of ambient temperatures and finding the maximum COP profile that can be achieved by the whole system. The proposed study extends the optimisation modelling of the chiller-AHUs system introduced in Zulkafli et al. (2022) with the effect of various ambient temperatures to obtain maximum COP profile for different time periods.

The optimisation modelling framework for the chiller-AHU system is formulated by combining the operational model for the chillers, AHU units, and cooling towers. The main goal of this study is to represent the interaction of various components in the system and to evaluate the power consumption, coefficient of performance (COP), and potential reduction in electricity bills with consideration of different ambient temperatures. The novelty and the primary impact of this paper are.

- Formulation of optimisation modelling as a linear programming model for the chiller-AHU system to obtain optimal decision solutions at the minimum electricity cost.
- The optimal solution shows improvement in comparison to the current operation of the chiller-AHU system in terms of power consumption, coefficient of performance (COP), and electricity cost.
- The percentage of improvement for COP is 7%–10%, with a reduction of power consumption and electricity cost of 1%–3%.

2. Optimisation problem statement

The optimal decision results for the chiller-AHU system of a building is the primary goal of the proposed optimisation framework. The components in the optimisation model that define the optimisation problems

Table 1
Lists of main contributions on the optimisation modelling of the chiller-AHU system.

Author	Chiller	AHU	Cooling Load	Cooling Demand	Methods	Energy consumption	COP	Weather condition
(Baakeem et al., 2018)	✓	X	✓	X	Conjugate direction method	✓	✓	X
(Kim et al., 2022)	✓	X	✓	X	Mixed-integer linear model	✓	X	X
(Kong et al., 2021)	✓	X	✓	X	Evolution algorithm	✓	✓	X
(Huang et al., 2018)	✓	X	✓	X	Monte-Carlo simulation	✓	✓	✓
(Nagraj et al., 2022)	✓	X	✓	X	Genetic algorithm	✓	✓	X
(Shao et al., 2019)	✓	X	✓	X	Accelerated particle swarm	✓	X	X
(Sun et al., 2020)	✓	X	✓	X	Regression neural network	✓	✓	✓
(Sadat-mohammadi et al., 2020)	✓	X	✓	X	Non-linear model	✓	✓	X
(Wang et al., 2022b)	✓	✓	✓	X	Non-linear model	✓	X	✓
(Zulkafli et al., 2022)	✓	✓	✓	✓	Linear model	✓	✓	X

of the chiller-AHU system are.

- i. The operational time ($t \in T$) of the chiller-AHU system is distributed equally for every 10 min time interval starting at 8:00 a.m. until 5:00 p.m.
- ii. The effectiveness (ϵ_i^{air}) and air mass flow rate ($\dot{m}_{(i,t)}^{air}$) for each operational time are defined for every cooling tower ($i \in I$).
- iii. The minimum and maximum levels for air mixed temperature (α_j^m), air supply temperature (α_j^s), mixed air moisture content (α_j^{mix}), supply air moisture content (α_j^{sh}), and the rate of change of ambient temperature ($\dot{t}_j^{mix, outside}$) are included for every air handling unit ($j \in J$).
- iv. The minimum and maximum levels for chilled water return temperature (α_k^r) and chilled water supply temperature (α_k^s), maximum cooling load ($q_{c(k)}^{max}$), and chilled water mass flow rate ($\dot{m}_{(k,t)}^{chw}$) are incorporated for every chiller ($k \in K$).
- v. The gradient coefficient ($\beta_{(k,t)}$) and intercept coefficient ($\gamma_{(k,t)}$) of power consumption for every chiller to the change of chilled water temperature is obtained from regression analysis.
- vi. The fixed electricity tariff rates (ϕ_t^{elec}) based on medium voltage commercial tariff and high penalty cost ($\phi_t^{penalty}$) are given.

The main objective of the optimisation model is to minimise the total electricity cost and to obtain the optimal decisions for the operation of the chiller-AHU system. The optimal solutions from the decision variables for the optimisation model are:

- i. The cooling capacity of an evaporator, heat rejection of the condenser and the power consumption of the compressor for every operational time.
- ii. The chilled water return and supply temperature of the chiller.
- iii. The partial load ratio of each chiller.
- iv. The sensible and latent heat, air mixed and supply temperature, and mixed and supply air moisture contents of the AHUs.
- v. The heat rejection capacity of the cooling tower.
- vi. The total cooling demand for all AHUs in the building.

3. Optimisation model for chiller-AHU system

The optimisation model for the chiller-AHU system is written as a linear programming model (LP). The optimisation model is adopted from the previous study (Zulkafli et al., 2022). In this study, a new set of values for parameters is obtained from the building management system (BMS), and the data collection for each chiller is from the installation of a power logger and flow meter.

There are four key parts of the optimisation model. The first part of the optimisation model is the cooling tower unit model, which accounts for the condenser's heat transfer balance, the cooling tower's effectiveness, and its heat rejection capacity. The second part of the optimisation model is the air handling units, which measure both the latent

heat of evaporation and the sensible heat of the building. The third part is the chiller system which relates to the cooling load and cooling demand of the building spaces. The last part of optimisation modelling describes the objective function to minimise the total electricity costs for the chiller-AHU system.

3.1. Cooling tower unit model

The function of a cooling tower is to reduce condenser water temperature by exchanging its heat with ambient air. The cooling tower's effectiveness is crucially affected by the conditions of ambient air and condenser water. The heat transfer balance for the condenser water cycle is defined in equation (1) (Zulkafli et al., 2022).

$$\sum_{i \in I} \dot{m}_{(i,t)}^{air} (h_i^{air, in} - h_i^{air, out}) = \sum_{j \in J} Q_{(j,t)}^{cdr} \quad \forall t \in T \quad (1)$$

The $\dot{m}_{(i,t)}^{air}$ is the mass flow rate of ambient air, $h_i^{air, in}$ is the enthalpy of inlet ambient air and $h_i^{air, out}$ is the enthalpy of outlet ambient air.

The cooling tower's effectiveness (ϵ_i^{air}) is considered in the heat rejection capacity of the cooling tower ($Q_{(i,t)}^{ct}$) according to equation (2).

$$Q_{(i,t)}^{ct} = \epsilon_i^{air} \dot{M}_{(i,t)}^{air} (h_i^{air, in} - h_i^{sat, air, in}) \quad \forall i \in I, t \in T \quad (2)$$

$$\dot{m}_{(i,t)}^{air, min} \leq \dot{M}_{(i,t)}^{air} \leq \dot{m}_{(i,t)}^{air, max} \quad \forall i \in I, t \in T \quad (3)$$

Equation (3) defines the mass flow rate of air is within the range of minimum ($\dot{m}_{(i,t)}^{air, min}$) and maximum ($\dot{m}_{(i,t)}^{air, max}$) air mass flow rate that enters the cooling tower. Equation (4) defines the effectiveness of the cooling tower.

$$\epsilon_i^{air} = \frac{T_i^{hot, water, in} - T_i^{cold, water, out}}{(T_i^{hot, water, in} - T_i^{wet, bulb})} \times 100 \quad (4)$$

3.2. Air handling unit model

The air handling unit (AHU) is intended to provide cooled air to the building spaces by exchanging the heat of the mixed hot air from the building spaces with the chilled water cycle from the chiller. There are two types of heat for building spaces, namely sensible heat ($SH_{(j,t)}$) as defined in equation (5), and latent heat ($LH_{(j,t)}$) as defined in equation (8). Sensible heat relates to the thermal energy exchange between the mixed hot air and the supply cold air.

$$SH_{(j,t)} = \dot{m}_{(j,t)}^{supply} c_j^{SH} (T_{(j,t)}^{mix} - T_{(j,t)}^{supply}) \quad \forall j \in J, t \in T \quad (5)$$

$$\alpha_j^{m, min} \leq T_{(j,t)}^{mix} \leq \alpha_j^{m, max} \quad \forall j \in J, t \in T \quad (6)$$

$$\alpha_j^{st, min} \leq T_{(j,t)}^{supply} \leq \alpha_j^{st, max} \quad \forall j \in J, t \in T \quad (7)$$

In equation (5), $\dot{m}_{(j,t)}^{supply}$ is the supply air flow rate from AHU to the room and c_j^{SH} is the sensible heat coefficient. The minimum and maximum

level for mixed air temperature ($T_{(j,t)}^{mix}$) is indicated as $\alpha_j^{m,min}$ and $\alpha_j^{m,max}$, respectively. The value of $\alpha_j^{st,min}$ and $\alpha_j^{st,max}$ shows the range of the minimum and maximum levels of supply air temperature ($T_{(j,t)}^{supply}$).

$$LH_{(j,t)} = \dot{m}_{(j)}^{supply} c_{j,LH} \left(M_{(j,t)}^{mix} - M_{(j,t)}^{supply} \right) \quad \forall k \in K, t \in T \quad (8)$$

$$\alpha_j^{mix,min} \leq M_{(j,t)}^{mix} \leq \alpha_j^{mix,max} \quad \forall k \in K, t \in T \quad (9)$$

$$\alpha_j^{sh,min} \leq M_{(j,t)}^{supply} \leq \alpha_j^{sh,max} \quad \forall k \in K, t \in T \quad (10)$$

The latent heat of evaporation is the heat required by the system to evaporate water using heat from the air while the energy in the air is maintained Equation (8) indicates the latent heat ($LH_{(j,t)}$) calculation involves the supply air mass flow rate ($\dot{m}_{(j)}^{supply}$), specific heat coefficient of air ($c_{j,LH}$), and the difference in humidity ratio for mixed air ($M_{(j,t)}^{mix}$) and supply air ($M_{(j,t)}^{supply}$) of the AHUs. The minimum ($\alpha_j^{mix,min}$) and maximum ($\alpha_j^{mix,max}$) bound for humidity ratio for mixed air are shown in equation (9) and the minimum ($\alpha_k^{sh,min}$) and maximum ($\alpha_k^{sh,max}$) bound for humidity ratio for supply air as in equation (10).

The total heat of the building is the total sensible heat and latent heat of all AHUs in the building as shown in equation (11).

$$Q_{(j,t)}^{building} = \sum_{j \in J, t \in T} (SH_{(j,t)} + LH_{(j,t)}) \quad \forall j \in J, t \in T \quad (11)$$

Equation (12) describes the temperature of the mixed air and the degree to which it rises or falls relative to the temperature of the surrounding air during normal hot and humid weather.

$$T_{(j,t)}^{mix} = tmix_j + t_{(j,t)}^{mix,outside} \quad \forall j \in J, t \in T : t = 1 \quad (12)$$

$$T_{(j,t)}^{mix} = T_{(j,t-1)}^{mix} + t_{(j,t)}^{mix,outside} \quad \forall j \in J, t \in T : t > 1$$

The initial mixed air temperature ($tmix_j$) is set only for the first time point of operational time. The mixed air temperature ($T_{(j,t)}^{mix}$) is influenced by the rate of change of the ambient air temperature ($t_{(j,t)}^{mix,outside}$) for every time point. This equation aims to simulate the fluctuations in ambient temperature outside the building and the mixed air temperature inside the building spaces.

3.3. Chiller unit model

Chillers are the key component of the chiller-AHU system. The chiller system composes of a compressor, evaporator, and condenser. The cooling load that is generated by the evaporator exchanges the heat of chilled water with the refrigerant. The cooling load of the chiller varies according to several factors, such as the size of the occupancy, the size of the building, and the outdoor ambient temperature. It is important to understand how the cooling load changes at different operational times. Equation (13) represents the cooling load of the evaporator ($Q_{(k,t)}^{evr}$) that consists of chilled water mass flowrates ($\dot{m}_{(k,t)}^{chw}$), the specific heat capacity of water (c_w), and the change in the circulation temperature of chilled water ($T_{(k,t)}^{rt} - T_{(k,t)}^{sp}$).

$$Q_{(k,t)}^{evr} = \dot{m}_{(k,t)}^{chw} c_w \left(T_{(k,t)}^{rt} - T_{(k,t)}^{sp} \right) \quad \forall k \in K, t \in T \quad (13)$$

$$Q_{(k,t)}^{cdr} = Q_{(k,t)}^{evr} + Q_{(k,t)}^{chiller} \quad \forall k \in K, t \in T \quad (14)$$

The heat rejection by the condenser ($Q_{(k,t)}^{cdr}$) is calculated by using the energy balance equation of the cooling load of the evaporator and power consumption of the compressor in the chiller system as defined in equation (14).

$$\alpha_k^{r,min} \leq T_{(k,t)}^{rt} \leq \alpha_k^{r,max} \quad \forall k \in K, t \in T \quad (15)$$

$$\alpha_k^{s,min} \leq T_{(k,t)}^{sp} \leq \alpha_k^{s,max} \quad \forall k \in K, t \in T \quad (16)$$

Equation (15) indicates the minimum ($\alpha_k^{r,min}$) and maximum ($\alpha_k^{r,max}$) temperature range of chilled water return ($T_{(j,t)}^{rt}$) and equation (16) indicates the minimum ($\alpha_k^{s,min}$) and maximum ($\alpha_k^{s,max}$) temperature range of chilled water supply temperature ($T_{(k,t)}^{sp}$).

The temperature of the chilled water returns to the chiller after it cools the building is called as the chilled water return temperature. The energy consumption of the chiller is affected by the partial load ratio and the chilled water return temperature as shown in equation (17).

$$T_{(k,t)}^{rt} = T_{(k,t)}^{sp} + \frac{PLR_{(k,t)} Q_{c(k)}^{max}}{\dot{m}_{(k,t)}^{chw} c_w} \quad \forall k \in K, t \in T \quad (17)$$

$$PLR_{(k,t)} = \frac{Q_{(k,t)}^{evr}}{q_{c(k)}^{max}} \quad \forall k \in K, t \in T \quad (18)$$

The partial load ratio ($PLR_{(k,t)}$) is the ratio of the actual cooling capacity ($Q_{(k,t)}^{evr}$) and maximum cooling capacity of the chiller ($q_{c(k)}^{max}$) as expressed in equation (18).

During the process of cooling, the power consumption of the chiller is closely associated to the temperature change of chilled water according to the study by Liu et al. (Lu et al., 2019) and Deng et al. (2015). Equation (19) defines the power consumption of the chiller ($Q_{(k,t)}^{chiller}$) along the operational time of chiller operation.

$$Q_{(k,t)}^{chiller} = \beta_{(k,t)} \left(T_{(k,t)}^{rt} - T_{(k,t)}^{sp} \right) + \gamma_{(k,t)} \quad \forall k \in K, t \in T \quad (19)$$

The gradient coefficient of power consumption ($\beta_{(k,t)}$) and the coefficient of power consumption ($\gamma_{(k,t)}$) are extracted from the regression analysis. The historical data of the cooling load is plotted against the temperature deviation of chilled water to get the value for the coefficients from the linear equation of a line.

Pumps are required to transport the circulating chilled water cycle and the condenser water cycle. The cooling water flow rate in the pump varies with the changes in the cooling capacity of the system. The volume flow rate (\dot{V}_k^{cw} and \dot{V}_k^{cd}), pumping head (H_k^{cwpump} and H_k^{cdpump}), and pump efficiency (η_k^{cwpump} and η_k^{cdpump}) are measured. The power consumption of the condenser water pump ($Q_{(k,t)}^{cdpump}$) and chilled water pump ($Q_{(k,t)}^{cwpump}$) is expressed in equations (20) and (21), respectively.

$$Q_{(k,t)}^{cdpump} = \frac{\delta_k \dot{V}_k^{cd} H_k^{cdpump}}{\eta_k^{cdpump}} \quad \forall k \in K, t \in T \quad (20)$$

$$Q_{(k,t)}^{cwpump} = \frac{\delta_k \dot{V}_k^{cw} H_k^{cwpump}}{\eta_k^{cwpump}} \quad \forall k \in K, t \in T \quad (21)$$

Equation (22) illustrates the relationship that exists between the cooling capacity of the evaporator $Q_{(k,t)}^{evr}$ (also known as the cooling supply), and the heat rejection by the building $Q_{(k)}^{building}$ (also known as the cooling demand). External cooling requirement (W_i) with high penalty cost is included in equation (21) to prevent the system from obtaining external cooling from other resources. For example, the external cooling requirement such as from the portable fans or air conditioners are needed to support the insufficient cooling from the HVAC system in the building. The total cooling demand of the building should be fully satisfied by the cooling load (Zulkaffi and Kopanos, 2017).

$$\sum_{k \in K} Q_{(k,t)}^{evr} = \sum_{j \in J} Q_{(j,t)}^{building} + W_i \quad \forall t \in T \quad (22)$$

3.4. Objective function to minimise electricity cost

In this study, the goal of the optimisation model is to minimise electricity costs for the chiller-AHU system by taking into account the electricity costs for power consumption of the chillers and the pumps. The penalty cost ($\varphi_t^{penalty}$) is also added to the objective function when external cooling is needed to cool the building. Equation (23) describes the total linear cost objective function.

$$Z = \min \left[\sum_{j \in I, t \in T} \varphi_t^{elec} (Q_{(j,t)}^{chiller} + Q_{(j,t)}^{cwpump} + Q_{(j,t)}^{cdpump}) + \sum_{i \in T} \varphi_t^{penalty} W_i \right] \quad (23)$$

The electricity prices for commercial building is denoted as (φ_t^{elec}). According to the tariff rates set by Tenaga Nasional Berhad (TNB) Malaysia, a fixed electricity tariff for commercial buildings is imposed (TNB. Pricing and Tariffs, 2023).

4. Results and discussion

The proposed optimisation model for the chiller-AHU system was implemented in a case study of the HVAC system in a building that comprises 2 chillers, 2 cooling towers, and 17 air handling units. The optimisation model for the case study was solved for each time point from 8:00 a.m. until 5:00 p.m. with 10 min time intervals. The case study of the chiller-AHU units system with consideration of ambient temperature is developed by dividing the time interval into three parts of a day:

the morning from 8:00 a.m. until 11:50 a.m., the early afternoon from 12:00 p.m. until 1:50 p.m., the late afternoon from 2:00 p.m. until 5:00 p.m. The time segregation is done in this case study to investigate the effect of different ambient temperatures on the COP of the chiller.

4.1. A case study description of a chiller-AHU system

Fig. 1 presents the illustrative diagram of the operational network of chiller-AHU system. The system consists of two cooling towers (i1 and i2), seventeen air handling units (j1 – j17), and two chillers (k1 and k2). The time point for a case study begins at t1 (8:00 a.m.) and ends at t55 (5:00 p.m.). The time interval for each time point is 10 min. Each chiller has three main sets of equipment the compressor, condenser, and evaporator. The compressor consumes electricity to increase the pressure and drives the refrigerant gas in a continuous refrigeration cycle. The refrigerant gas is cooled in the condenser where heat is rejected to the condenser water cycle. The refrigerant is turned from gas to liquid in the condenser. The hot condenser water in the cooling tower is cooled by rejecting its heat to the surrounding air. Before the refrigerant returns to the compressor, the refrigerant absorbs heat from the chilled water inlet in the evaporator and the refrigerant will be evaporated. In the building, the hot air enters AHU to exchange its heat with a chilled water outlet. The cooled air leaves the AHU and returns to the building spaces to provide cooling for the building. This process continues throughout the air-conditioning time.

The list of main parameters for chiller units (k1 and k2) and cooling

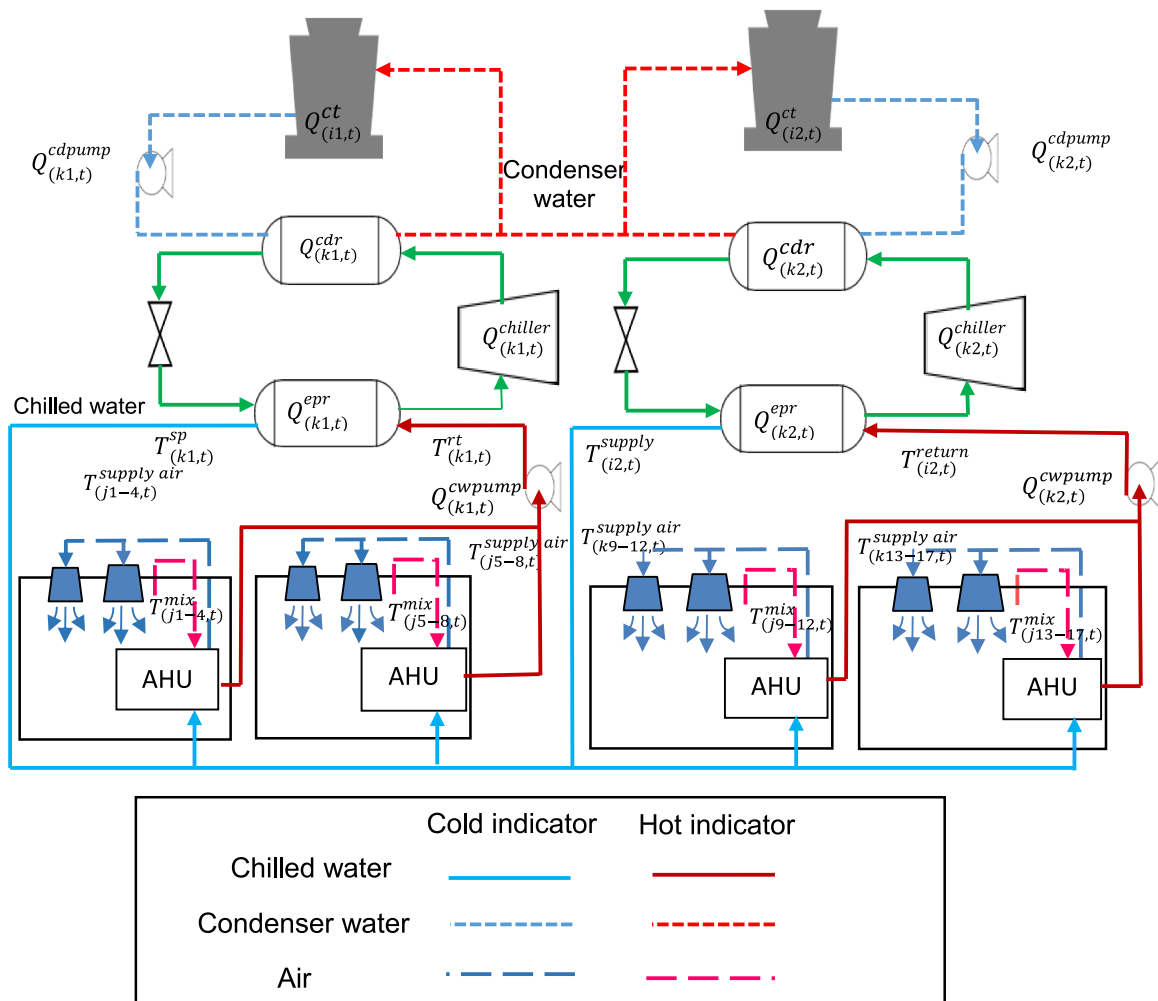


Fig. 1. Illustrative diagram of the network operation of the chiller-AHU system.

tower units ($j1 - j17$) is shown in Table 2. Note that, two set of values for each parameter for chiller units is displayed. The case study input parameters are obtained from the historical data of the building management system (BMS) in the university building and the information from the energy audit report. The electricity price is USD 0.0083/kWh according to the electricity tariff rates (tariff C1) for medium voltage commercial buildings (Berhad, 2014).

Fig. 2 shows the chilled water mass flow rate for chiller k1 and k2 for the whole duration of the chiller operation in a day. The value for the mass flow rate is calculated from the chilled water velocity that is obtained from the BMS with a known cross-sectional area of the pipe and the density of water.

Fig. 3 presents the gradient coefficient of power consumption and Fig. 4 shows the intercept coefficient of power consumption for each chiller. The values of these coefficients are obtained from the linear regression between the power input and the chilled water temperature deviation. The linear regression analysis is done according to the three cases of weather conditions which are in the morning, early afternoon, and late afternoon. According to the published work of Salari et al. (Salari and Askarzadeh, 2015), the power coefficient of the chiller depends on chilled water temperature deviation. Although the equation

can be derived as a polynomial equation, to maintain linear model formulation, the linear equation is obtained by interpolating these two variables with a coefficient of determination (R-Squared) above 80% for all the cases.

Table 3 lists all input parameters for air handling units, such as the supply air mass flow rate from AHU to the building spaces, the air temperature, and the humidity ratio. The supply air mass flow rate is calculated by measuring the velocity of air that enters the AHU. The mixed and supply air temperature is obtained from historical data in the BMS. Finally, the value of the humidity ratio is obtained by referring to the online interactive psychrometric chart (FlyCarpet Inc, 2023) by setting input data for air properties, which are the dry air temperature and the relative humidity, to get the value of the humidity ratio.

4.2. Results analysis of the case study

The case study of the chiller-AHU system in the building has been solved from equation (1) until (22) with the objective function of minimising the electricity cost of the system (equation (23)). The optimisation modelling is written as linear programming (LP) model in GAMS version 38.2 and solved by a CPLEX solver in an Intel(R) Core (TM) i7. The optimal results are analysed and discussed in this section.

Fig. 5 shows the deviation of chilled water temperature and the partial load ratio (PLR) of the chiller. The ratio of the current cooling load and the maximum cooling load is defined as the PLR. The maximum PLR for chiller k1 is at 12:20 p.m. and for chiller k2 is at 3:00 p.m. The PLR for chiller k1 reduces due to lower cooling load, but the PLR for chiller k2 shows the opposite trend at time 14:00. The current cooling load changes at this time point due to the changes in the power consumption profile (refer to Fig. 7). The chilled water return temperature ($T_{(k,t)}^r$) is influenced by the partial load ratio and minimum and maximum limit of the chilled water return and supply temperature according to equations (15)–(17).

Fig. 6 shows the comparison of normalised percentage analysis of cooling load, power input, and condenser load for chiller k1 and k2, respectively. The normalised percentage of a chiller is calculated as the fraction of the current value and the maximum value for each category. The power consumption profile follows the trend of the power coefficient in Figs. 3 and 4. For example, the power input for chiller k1 is reduced at 12:00 because the value for the beta coefficient (Fig. 3) is lower than the previous time point. On the other hand, the power input for chiller k2 is increasing at 14:00 because the gamma coefficient (Fig. 4) is higher than the previous time. The cooling load profile is affected by the power consumption, condenser load, and partial load ratio. The cooling load for chiller k1 is reduced at 14:00 h because the partial load ratio (Fig. 5) and chilled water temperature deviation (Fig. 6) are also reduced at the same time. Generally, the power input trend for chiller k1 and k2 follow similar trends of cooling load and condenser load profiles according to equation (14).

Fig. 7 displays the normalised percentage of the total cooling demand profile for chiller-AHU system. The normalised percentage is the fraction of the current cooling demand with the maximum cooling demand. The total cooling demand is taken as the total heat rejected in the building by measuring the total sensible and latent heat of the building (equation (11)). At the beginning of the chiller operation, the total cooling demand is expected to be high at around 98.5% due to the starting up of the operation of the chillers to initially reduce the chilled water temperature from ambient temperature to the desired cooling temperature. After the desired cooling temperature has been achieved, the total cooling demand is gradually declining until the time when the weather temperature outside the building is relatively high, especially in the early afternoon. The total cooling demand continues to increase until achieving the maximum normalised percentage of cooling demand which is at 100% at 15:00 h. After this hour, there is a slightly reducing trend of the cooling demand profile because the total sensible and latent

Table 2
List of main parameters for chiller units and cooling tower units.

Parameter	Description	Chiller (k1)/ Cooling tower	Chiller (k2)/ Cooling tower	Metric unit
$h_i^{air,in}$	enthalpy of air enters the cooling tower	309.84	309.84	kJ/kg
$h_i^{air,out}$	enthalpy of air leaves the cooling tower	299.7	299.7	kJ/kg
$h_i^{sat,air,in}$	enthalpy of saturation air	307.83	309.34	kJ/kg
$\dot{m}_{(i)}^{air,min}$	minimum air mass flow rate	20	20	kg/s
$\dot{m}_{(i)}^{air,max}$	maximum air mass flow rate	50	50	kg/s
ϵ_i^{air}	heat transfer effectiveness of cooling tower	0.173	0.133	–
c_w	specific heat of water	4.18	4.18	kJ/kg.°C
$q_{c(k)}^{max}$	maximum cooling capacity of chiller	623	432	kg/s
$\alpha_k^{r,min}$	minimum chilled water return temperature	12.17	12.34	°C
$\alpha_k^{r,max}$	maximum chilled water return temperature	14.62	14.47	°C
$\alpha_k^{s,min}$	minimum chilled water supply temperature	7.14	6.85	°C
$\alpha_k^{s,max}$	Maximum chilled water supply temperature	8.12	7.70	°C
\dot{V}_k^{cw}	volume flow rate of chilled water	0.079	0.078	m ³ /s
\dot{V}_k^{cd}	volume flow rate of condenser water	0.078	0.078	m ³ /s
H_k^{cwpump}	pumping head of chilled water pump	19.8	19.8	m
H_k^{cdpump}	pumping head of condenser water pump	19.8	19.8	m
η_k^{cwpump}	chilled water pump efficiency	0.78	0.78	–
η_k^{cdpump}	condenser water pump efficiency	0.58	0.56	–
c_p^{SH}	specific heat of air	j1 - j17	1.21	kJ/kg.°C
c_p^{LH}	latent heat of vaporisation	j1 - j17	3000	kJ/kg

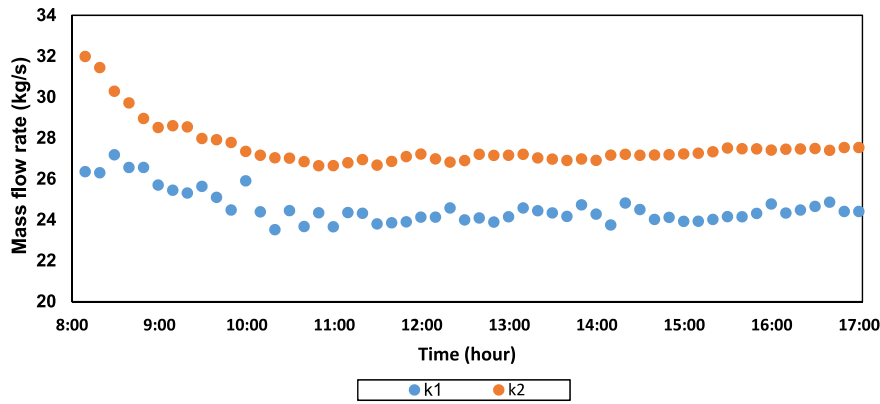


Fig. 2. Chilled water mass flow rate for each chiller unit.

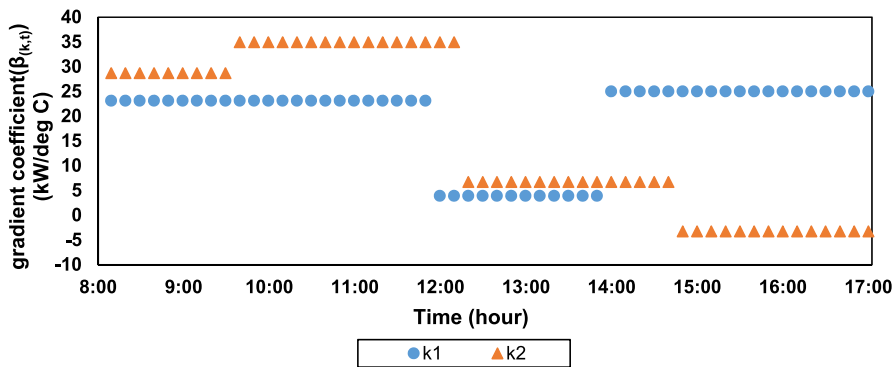


Fig. 3. The value for the gradient coefficient for each chiller over a time horizon.

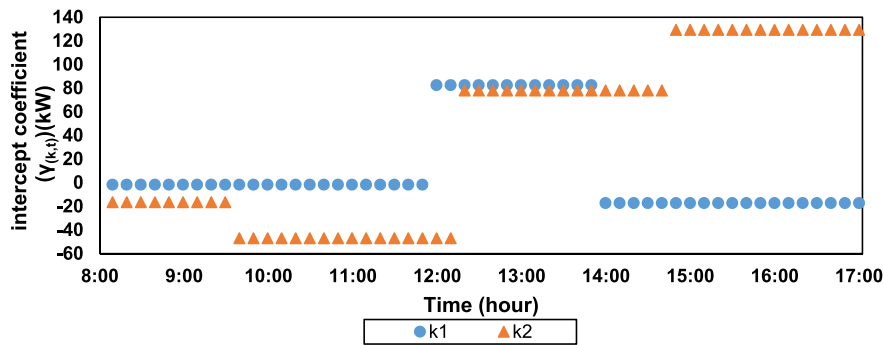


Fig. 4. The value for the intercept coefficient for each chiller over a time horizon.

heat are slightly reduced (Figs. 8 and 9) towards the end of the chiller-AHU operation. According to equation (22), the total cooling demand profile of the building in Fig. 7 should be the same as the cooling load of the chillers.

The sensible heat and latent heat profiles for all AHUs in the building are shown in Figs. 8 and 9, respectively. The sensible heat profile is generally higher than the latent heat because the exchange of thermal energy between mixed hot air and supply cold air is usually higher than the heat released by the system during the constant-temperature process. The profile trend for both sensible and latent heat shows a similar trend to the total cooling demand profile.

Fig. 10 displays the power consumption comparison in the chiller-AHU system. The total power consumption of the chiller-AHU system consists of the power input of the chiller, chilled water pump, and

condenser water pump. The optimal chiller-AHU operation from the results solution and the current chiller operation from the energy audit report are compared. The percentage gap between the power consumption of the optimal and the current chiller k1 and k2 are 3% and 1%, respectively. The same pattern is observed for the current and optimal electricity cost for both chillers because electricity cost is calculated by multiplying the power consumption with the fixed value of the electricity tariff (Berhad, 2014).

Fig. 11 presents the optimal COP profile for each chiller throughout the chiller-AHU operation. COP is the ratio of the cooling load and the power consumption of the chiller. The high value of COP indicates efficient chiller performance to produce maximum cooling load with the minimum power consumption of the chiller and vice versa. The average optimal COP for both chillers in the morning is about the same, with a

Table 3
Air flow rate, air temperature, and humidity ratio for AHU.

AHU	$\dot{m}_{(j)}^{supply}$ (kg/s)	$\alpha_j^{m,min}$ (°C)	$\alpha_j^{m,max}$ (°C)	$\alpha_j^{st,min}$ (°C)	$\alpha_j^{st,max}$ (°C)	$\alpha_j^{mix,min}$	$\alpha_j^{mix,max}$	$\alpha_j^{sh,min}$	$\alpha_j^{sh,max}$
j1	8.612	21	22.1	14.8	20.4	0.011	0.012	0.008	0.010
j2	8.395	23	24.5	15.1	20.8	0.013	0.015	0.009	0.013
j3	4.373	24	25.6	17.8	21.0	0.015	0.017	0.011	0.015
j4	4.929	24	24.7	13.0	20.9	0.015	0.016	0.008	0.015
j5	4.130	23	25.9	15.6	22.4	0.014	0.018	0.009	0.013
j6	7.040	26	27.5	19.3	21.5	0.016	0.020	0.011	0.015
j7	7.040	24	26.0	13.3	21.3	0.014	0.017	0.007	0.014
j8	4.450	22	26.8	11.1	17.0	0.012	0.018	0.006	0.012
j9	6.044	25	28.8	11.6	21.2	0.014	0.019	0.007	0.014
j10	3.822	23	27.3	11.4	21.0	0.015	0.020	0.007	0.014
j11	3.703	23	25.6	14.4	21.6	0.015	0.019	0.009	0.015
j12	2.003	23	28.9	12.7	19.7	0.014	0.024	0.007	0.014
j13	3.185	24	26.1	17.0	21.4	0.015	0.018	0.010	0.015
j14	9.262	25	27.4	9.9	20.2	0.014	0.016	0.006	0.013
j15	9.012	25	27.3	9.6	20.1	0.014	0.016	0.006	0.013
j16	6.892	24	25.0	12.3	21.3	0.014	0.014	0.007	0.013
j17	8.823	25	25.8	12.1	21.1	0.014	0.015	0.007	0.013

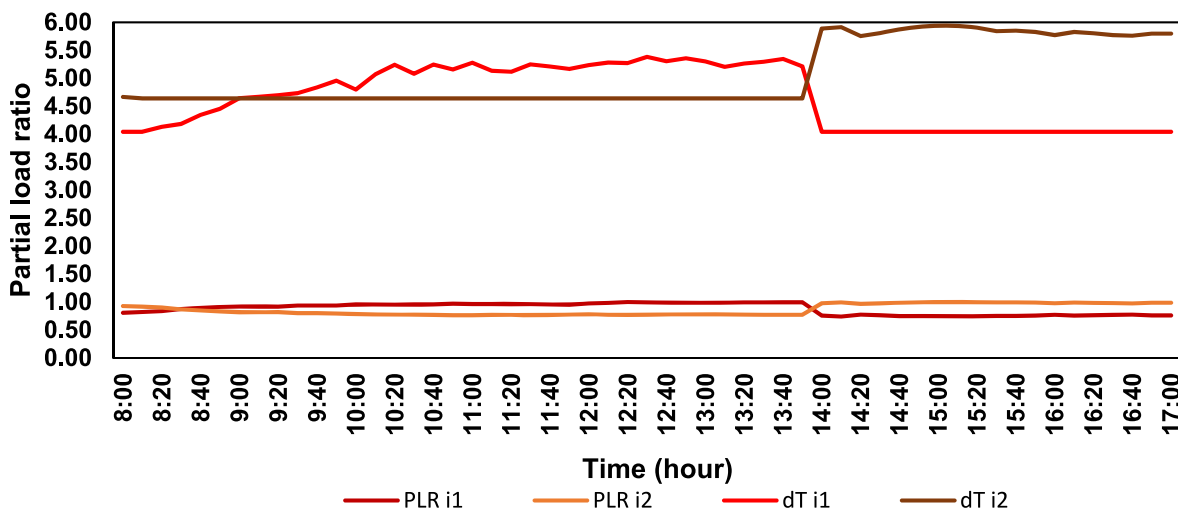


Fig. 5. Partial load ratio and chilled water temperature deviation for each chiller.

COP of around 4.7 to 4.9. In the early afternoon, COP for chiller k1 is higher than the chiller k2 because the cooling load for k1 is generally high relative to decreased power consumption (Fig. 6). The COP for chiller k2 increased in the late afternoon with the average optimal COP of 5.96 due to the same reason.

Table 4 presents the comparison of optimal and current average COP for each chiller. The optimal COP is obtained from the optimal solution of the optimisation modelling of the chiller-AHU system. The current COP is calculated from the historical data collection of the cooling load and power input of the chiller. In general, the optimal COP for both chillers is higher than the current COP. The average optimal COP for k1 is 4.95 and for k2 is 5.21. According to the ASHRAE chiller plant efficiency chart (Hartman, 2001), the COP above 4.8 indicates a high-efficiency optimised chiller plant. The percentage difference for chiller k1 and k2 are 7.3% and 10% improvement, respectively. This percentage difference may represent a potential capability solution from the optimisation modelling of the chiller-AHU system to increase the efficiency of the actual chiller operation.

The proposed potential solution can be in terms of controlling the percentage of valve opening of the chilled water flow rates from the building management system (BMS) to regulate the chilled water temperature and set the desired range value of the chilled water supply temperature. The comparison of the optimal and current average chilled water return and supply temperature is shown in Table 5 and Table 6, respectively. The main parameter to observe is the chilled water

temperature deviation between the chilled water return and supply temperature. The chilled water temperature deviation (dT) for chiller k1 and k2 for optimal operation is greater than that of the current chiller operation. The higher value of temperature deviation means that the cooling load of the chiller will be higher at specified chilled water mass flow rates while maintaining the minimum power consumption of the chiller. As a result, a high COP value is obtained according to Table 3.

As discussed previously, the optimal decision results are generated and analysed to search for the potential capability of the system to implement optimal decision solutions. The main objective of the developed optimisation model of the chiller-AHU system is to minimise electricity cost and obtain the maximum value of COP. If the actual system is capable to follow the proposed optimal decision from the model solutions, the potential of minimising the electricity bill in comparison to the previous chiller-AHU operation will be significantly realised because the minimum benchmark of the optimised cost is known from the model solutions. The next step is to set up an on-site demonstration of the chiller-AHU system by testing potential parameters in the BMS of the chiller-AHU system according to the optimised results for a few weeks or months. The performance evaluation in terms of electricity cost and COP calculation will be completed to analyse the comparison of the current set point values with the optimal set point values. Additionally, the site demonstration will be successful if the minimum electricity bill can be established and a high value of COP can be acquired (Kim et al., 2022).

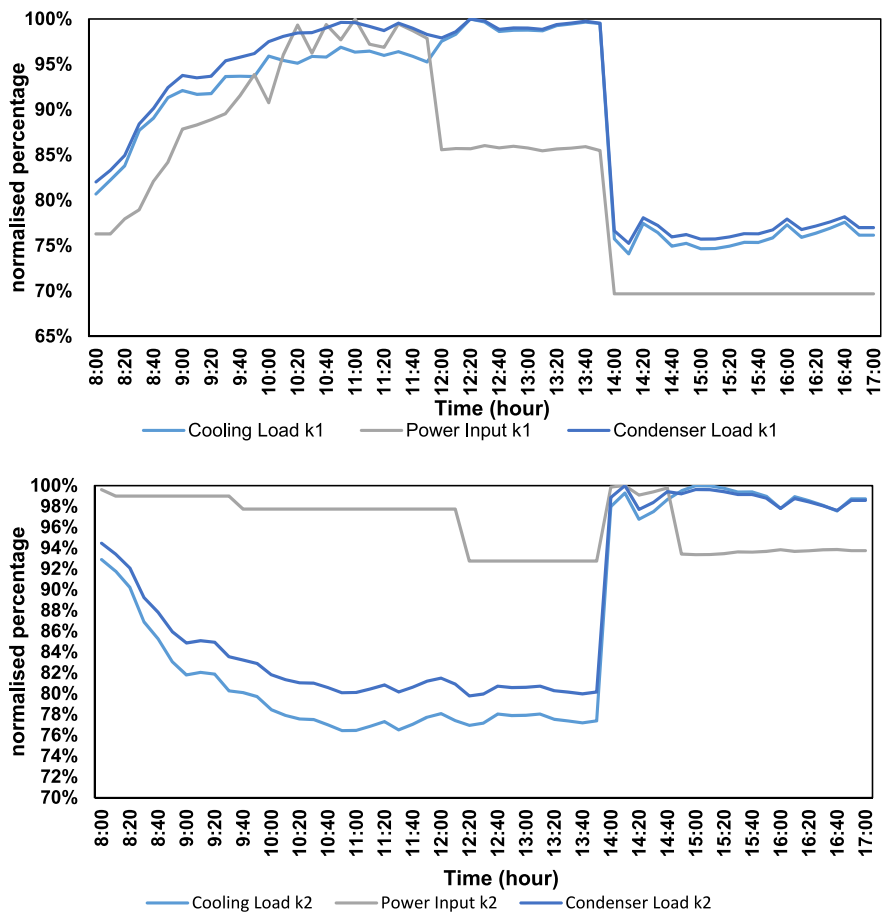


Fig. 6. Cooling load, power input, and condenser load for each chiller.

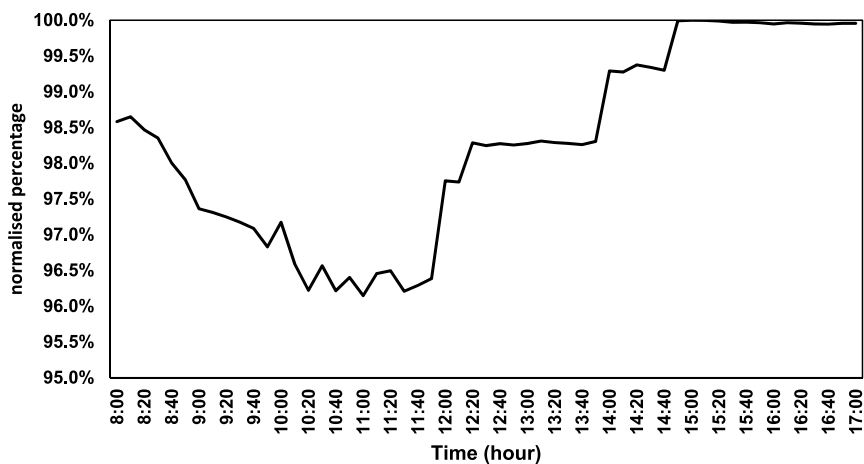


Fig. 7. Total cooling demand profile for Chiller-AHU operation in a day.

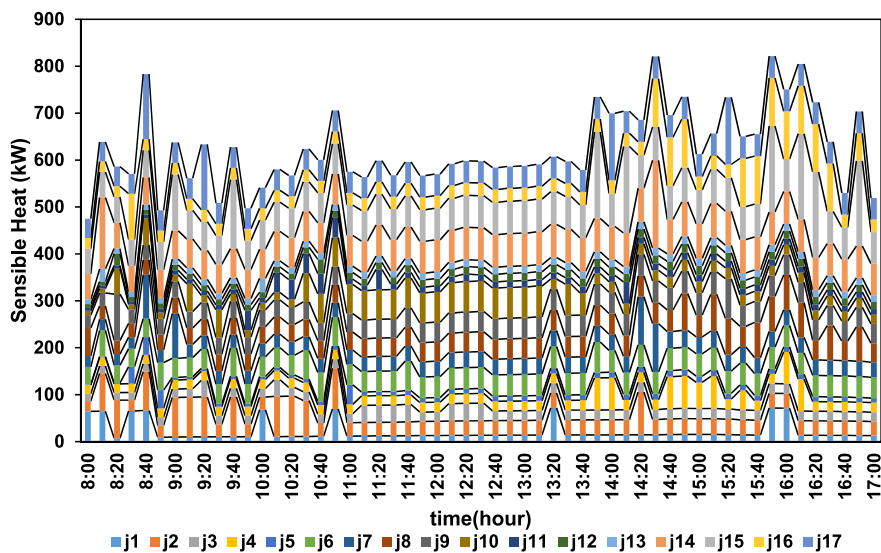


Fig. 8. Sensible heat profile.

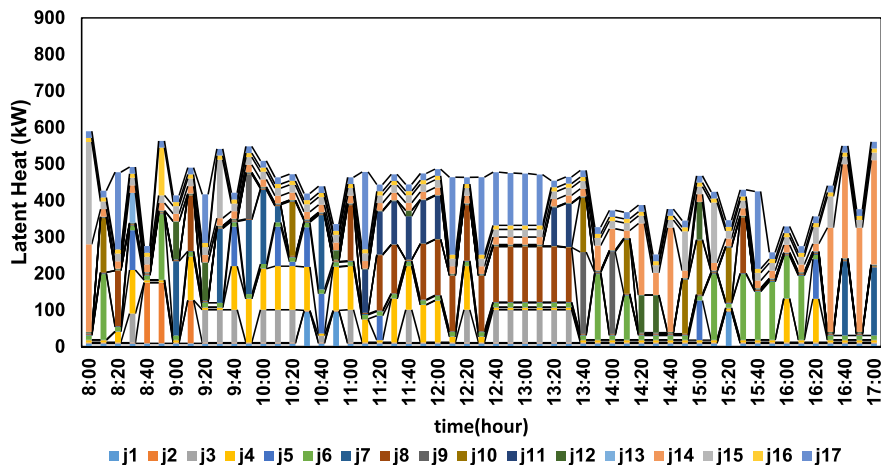


Fig. 9. Latent heat profile.

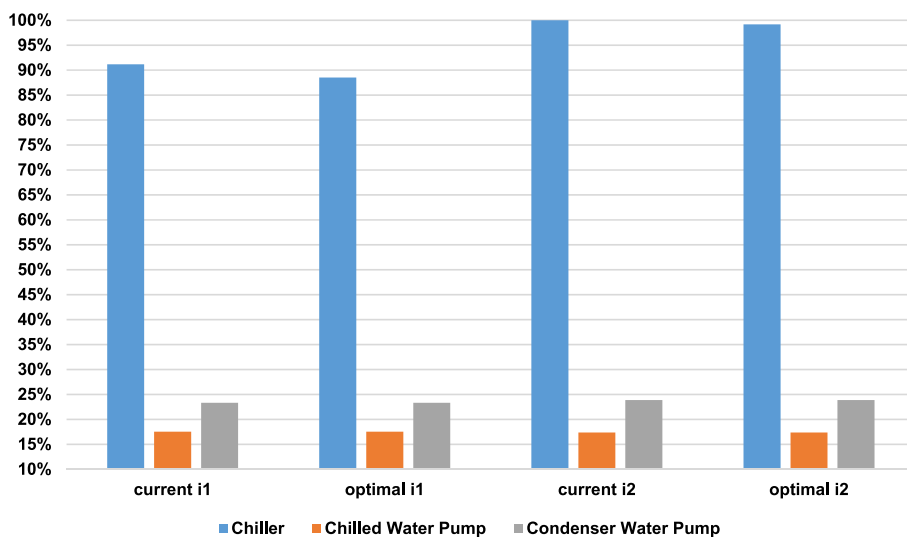


Fig. 10. Power consumption comparison of optimal and current chiller operation.

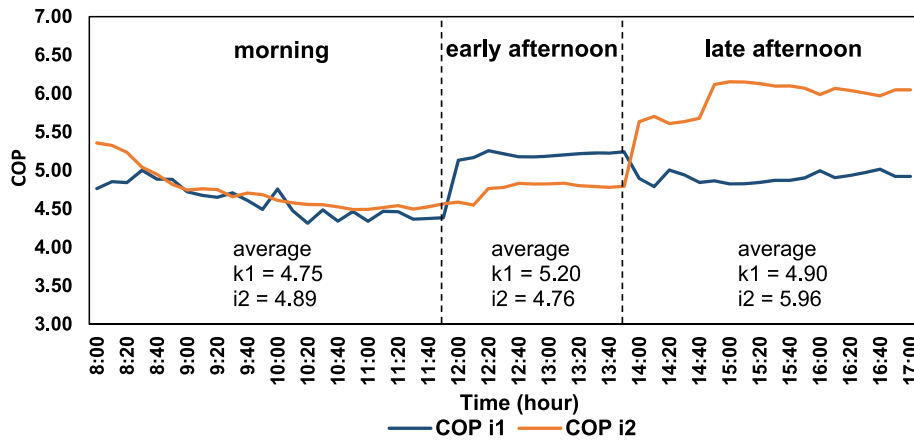


Fig. 11. Optimal COP profile for each chiller.

Table 4

COP comparison for the chiller-AHU system based on different cases of the surrounding temperature.

Case	Morning	Early Afternoon	Late Afternoon	Average
Current k1	4.49	4.67	4.65	4.61
Optimal k1	4.75	5.20	4.90	4.95
Current k2	4.71	4.75	4.75	4.74
Optimal k2	4.89	4.76	5.96	5.21

5. Conclusion

In developing an optimisation model for the chiller-AHU system, the modelling interaction of each set of equipment must be considered in representing the actual cooling process of a building under a wide range of ambient temperatures. The whole chiller-AHU system, which is composed of the cooling tower system, chiller network, and air handling units were properly modelled in this study by accounting for different ambient condition, which is in the morning, early afternoon, and late afternoon. For realising optimal operation, correlation analysis of the

empirical data of power consumption and temperature deviation of chilled water cycle under different weather conditions was investigated to predict the chiller power consumption. An AHU model was developed based on the mixed air temperature, which varied with ambient temperature, and the cooling tower model accounted for the cooling tower's effectiveness under different ambient conditions.

This study showed that the performance of the current chiller-AHU system in the building can be further improved by about 7–10%. To achieve the optimal COP, the chilled water temperature for the chiller and return air temperature for AHU can be set in the BMS or at the on-site plant by following the optimal decisions. However, the pragmatic approach to test whether the optimal decisions of the chiller-AHU model is capable of reducing electricity bills is by implementing onsite demonstration in the real chiller-AHU system of the building. Further analysis of the performance evaluation is needed to prove that the optimal decision from the solution of the chiller-AHU model is indeed more efficient than the current practice. Nevertheless, this study can be a baseline for obtaining a high energy star rating for the green building by minimising energy consumption to ensure sustainable energy practices in the building.

Table 5

Optimal and current chilled water return and supply temperature for chiller k1.

Case	Morning (°C)	Early Afternoon(°C)	Late Afternoon (°C)	Average(°C)
Current $T_{(k1,t)}^r$	12.90	12.17	12.36	12.48
Current $T_{(k1,t)}^{sp}$	8.74	8.20	8.52	8.49
dT k1	4.16	3.97	3.84	3.99
Optimal $T_{(k1,t)}^r$	12.23	12.42	12.16	12.27
Optimal $T_{(k1,t)}^{sp}$	7.42	7.14	8.12	7.56
dT k2	4.81	5.28	4.04	4.71

Table 6

Optimal and current chilled water return and supply temperature for chiller k2.

Case	Morning (°C)	Early Afternoon (°C)	Late Afternoon (°C)	Average(°C)
Current $T_{(k2,t)}^r$	12.77	12.34	12.84	12.65
Current $T_{(k2,t)}^{sp}$	8.41	7.79	8.13	8.11
dT k1	4.36	4.55	4.71	4.54
Optimal $T_{(k2,t)}^r$	12.34	12.34	12.68	12.45
Optimal $T_{(k2,t)}^{sp}$	7.70	7.70	6.85	7.42
dT k2	4.64	4.64	5.83	5.03

Declaration of competing interest

The authors declare that they have no known competing financial interests or personal relationships that could have appeared to influence the work reported in this paper.

Data availability

Data will be made available on request.

NOMENCLATURE

Indices and Sets

$i \in I$	cooling tower
$j \in J$	air handling unit
$k \in K$	chiller
$t \in T$	time

Parameters

$\alpha_j^{m,min}$	minimum air mixed temperature ($^{\circ}\text{C}$)
$\alpha_j^{m,max}$	maximum air mixed temperature ($^{\circ}\text{C}$)
$\alpha_j^{mix,min}$	minimum mixed air moisture content
$\alpha_j^{mix,max}$	maximum mixed air moisture content
$\alpha_j^{st,min}$	minimum supply air temperature ($^{\circ}\text{C}$)
$\alpha_j^{st,max}$	maximum supply air temperature ($^{\circ}\text{C}$)
$\alpha_j^{sh,min}$	minimum supply air humidity ratio
$\alpha_j^{sh,max}$	maximum supply air humidity ratio
$\alpha_k^{r,min}$	minimum chilled water return temperature ($^{\circ}\text{C}$)
$\alpha_k^{r,max}$	maximum chilled water return temperature ($^{\circ}\text{C}$)
$\alpha_k^{s,min}$	minimum chilled water supply temperature ($^{\circ}\text{C}$)
$\alpha_k^{s,max}$	maximum chilled water supply temperature ($^{\circ}\text{C}$)
$\beta_{(k,t)}$	gradient coefficient of power consumption ($\text{kW}/^{\circ}\text{C}$)
c_j^{SH}	specific heat of air ($\text{kJ}/\text{kg}\cdot\text{K}$)
c_j^{LH}	latent heat of vaporisation (kJ/kg)
c_w	specific heat of water ($\text{kJ}/\text{kg}\cdot\text{K}$)
δ_k	specific weight of water
$\gamma_{(k,t)}$	intercept coefficient of power consumption (kW)
ε_t^{air}	heat transfer effectiveness of cooling tower
$h_i^{air,in}$	enthalpy of air enters the cooling tower (kJ)
$h_i^{air,out}$	enthalpy of air leaves the cooling tower (kJ)
$h_i^{sat,air,in}$	enthalpy of saturation air based on temperature of water entering the cooling tower (kJ)
H_k^{cwpump}	pumping head of chilled water pump (m)
H_k^{cdpump}	pumping head of condenser water pump (m)
$\dot{m}_{(i)}^{air,min}$	minimum air mass flow rate (kg/s)
$\dot{m}_{(i)}^{air,max}$	maximum air mass flow rate (kg/s)
$\dot{m}_{(k,t)}^{chw}$	chilled water mass flowrate (kg/s)
$\dot{m}_{(j)}^{supply}$	supply air flow rate from AHU to room (kg/s)
η_k^{cwpump}	chilled water pump efficiency
η_k^{cdpump}	condenser water pump efficiency
φ_t^{elec}	electricity prices ($\$/\text{kW}$)
$\varphi_t^{penalty}$	penalty cost ($\$/\text{kW}$)
$l_{(j,t)}^{mix,outside}$	degree of changes of the ambient temperature ($^{\circ}\text{C}$)
$Q_{c(k)}^{max}$	maximum cooling capacity of chiller (kW)
\dot{V}_k^{cw}	volume flow rate of chilled water (m^3/s)
\dot{V}_k^{cd}	volume flow rate of condenser water (m^3/s)

Acknowledgment

This study is supported by the Universiti Teknikal Malaysia Melaka for giving financial and research support through the Short Term Research Grant (PJP/2021/FKM/S01809).

Decision Variables

- $LH_{(j,t)}$ latent heat of AHU (kW)
- $\dot{M}_{(i,t)}^{air}$ mass flowrate of air enters the cooling tower (kg/s)
- $M_{(j,t)}^{mix}$ humidity ratio of mixed air
- $M_{(j,t)}^{supply}$ humidity ratio of supply air
- $PLR_{(k,t)}$ partial load ratio
- $Q_{(j,t)}^{building}$ total heat rejection capacity in the building (kW)
- $Q_{(k,t)}^{chiller}$ power consumption of the chiller (kW)
- $Q_{(j,t)}^{cdr}$ heat transfer of the condenser (kW)
- $Q_{(i,t)}^{ct}$ heat rejection capacity of cooling tower (kW)
- $Q_{(k,t)}^{spr}$ cooling load of the evaporator in the chiller (kW)
- $Q_{(k,t)}^{cwpump}$ power consumption of chilled water pump (kW)
- $Q_{(k,t)}^{cdpump}$ power consumption of condenser water pump (kW)
- $SH_{(j,t)}$ sensible heat of AHU (kW)
- $T_{(j,t)}^{mix}$ air mixed temperature (°C)
- $T_{(j,t)}^{supply}$ air supply temperature (°C)
- $T_{(k,t)}^{rt}$ chilled water return temperature (°C)
- $T_{(k,t)}^{sp}$ chilled water supply temperature (°C)
- W_t penalty value due to insufficient cooling load (kW)

Appendix

A. Data for chilled water mass flow rate, $\dot{m}_{(k,t)}^{chw}$ (kg/s) for each chiller unit

Time period (t)	Chiller k1	Chiller k2
8:00:00	25.8568	32.19596
8:10:00	26.34833	31.98258
8:20:00	26.29524	31.43965
8:30:00	27.1729	30.28384
8:40:00	26.55408	29.71061
8:50:00	26.55922	28.95051
9:00:00	25.69266	28.50581
9:10:00	25.44458	28.59495
9:20:00	25.30525	28.53561
9:30:00	25.62921	27.97323
9:40:00	25.09253	27.91389
9:50:00	24.47216	27.77929
10:00:00	25.9019	27.34293
10:10:00	24.38572	27.15051
10:20:00	23.51356	27.02929
10:30:00	24.44489	27.01187
10:40:00	23.66474	26.83838
10:50:00	24.34029	26.63965
11:00:00	23.65722	26.64722
11:10:00	24.351	26.78788
11:20:00	24.31667	26.94141
11:30:00	23.79748	26.66591
11:40:00	23.84851	26.85328
11:50:00	23.8956	27.08434
12:00:00	24.12821	27.20934
12:10:00	24.12445	26.97801
12:20:00	24.57625	26.81759
12:30:00	23.99387	26.89005
12:40:00	24.08828	27.1963
12:50:00	23.88563	27.14398
13:00:00	24.1458	27.15202
13:10:00	24.57742	27.19722
13:20:00	24.43706	27.0197
13:30:00	24.33317	26.96465
13:40:00	24.16067	26.89874
13:50:00	24.72648	26.96869
14:00:00	24.27432	26.90429
14:10:00	23.74466	27.15581
14:20:00	24.81633	27.19672
14:30:00	24.50114	27.15429
14:40:00	24.01397	27.16465

(continued on next page)

(continued)

Time period (t)	Chiller k1	Chiller k2
14:50:00	24.11524	27.18258
15:00:00	23.9207	27.21818
15:10:00	23.92861	27.25
15:20:00	24.01432	27.32323
15:30:00	24.14836	27.50707
15:40:00	24.14575	27.46995
15:50:00	24.30999	27.46465
16:00:00	24.76669	27.4053
16:10:00	24.32691	27.44773
16:20:00	24.47221	27.46136
16:30:00	24.65094	27.48131
17:00:00	24.85903	27.39242

B. The value for the gradient coefficient, $\beta_{(k,t)}$ (kW/°C) for each chiller over a time horizon

Time period (t)	Chiller k1	Chiller k2
8:00:00	23.114	28.677
8:10:00	23.114	28.677
8:20:00	23.114	28.677
8:30:00	23.114	28.677
8:40:00	23.114	28.677
8:50:00	23.114	28.677
9:00:00	23.114	28.677
9:10:00	23.114	28.677
9:20:00	23.114	28.677
9:30:00	23.114	28.677
9:40:00	23.114	34.918
9:50:00	23.114	34.918
10:00:00	23.114	34.918
10:10:00	23.114	34.918
10:20:00	23.114	34.918
10:30:00	23.114	34.918
10:40:00	23.114	34.918
10:50:00	23.114	34.918
11:00:00	23.114	34.918
11:10:00	23.114	34.918
11:20:00	23.114	34.918
11:30:00	23.114	34.918
11:40:00	23.114	34.918
11:50:00	23.114	34.918
12:00:00	3.8923	34.918
12:10:00	3.8923	34.918
12:20:00	3.8923	6.7076
12:30:00	3.8923	6.7076
12:40:00	3.8923	6.7076
12:50:00	3.8923	6.7076
13:00:00	3.8923	6.7076
13:10:00	3.8923	6.7076
13:20:00	3.8923	6.7076
13:30:00	3.8923	6.7076
13:40:00	3.8923	6.7076
13:50:00	3.8923	6.7076
14:00:00	25	6.7076
14:10:00	25	6.7076
14:20:00	25	6.7076
14:30:00	25	6.7076
14:40:00	25	6.7076
14:50:00	25	-3.2812
15:00:00	25	-3.2812
15:10:00	25	-3.2812
15:20:00	25	-3.2812
15:30:00	25	-3.2812
15:40:00	25	-3.2812
15:50:00	25	-3.2812
16:00:00	25	-3.2812
16:10:00	25	-3.2812
16:20:00	25	-3.2812
16:30:00	25	-3.2812
16:40:00	25	-3.2812
16:50:00	25	-3.2812
17:00:00	25	-3.2812

C. The value for the intercept coefficient, $\gamma_{(k,t)}$ (kW) for each chiller over a time horizon

Time period (t)	Chiller k1	Chiller k2
8:00:00	-1.7307	-16.577
8:10:00	-1.7307	-16.577
8:20:00	-1.7307	-16.577
8:30:00	-1.7307	-16.577
8:40:00	-1.7307	-16.577
8:50:00	-1.7307	-16.577
9:00:00	-1.7307	-16.577
9:10:00	-1.7307	-16.577
9:20:00	-1.7307	-16.577
9:30:00	-1.7307	-16.577
9:40:00	-1.7307	-46.999
9:50:00	-1.7307	-46.999
10:00:00	-1.7307	-46.999
10:10:00	-1.7307	-46.999
10:20:00	-1.7307	-46.999
10:30:00	-1.7307	-46.999
10:40:00	-1.7307	-46.999
10:50:00	-1.7307	-46.999
11:00:00	-1.7307	-46.999
11:10:00	-1.7307	-46.999
11:20:00	-1.7307	-46.999
11:30:00	-1.7307	-46.999
11:40:00	-1.7307	-46.999
11:50:00	-1.7307	-46.999
12:00:00	82.509	-46.999
12:10:00	82.509	-46.999
12:20:00	82.509	78.012
12:30:00	82.509	78.012
12:40:00	82.509	78.012
12:50:00	82.509	78.012
13:00:00	82.509	78.012
13:10:00	82.509	78.012
13:20:00	82.509	78.012
13:30:00	82.509	78.012
13:40:00	82.509	78.012
13:50:00	82.509	78.012
14:00:00	-17.3	78.012
14:10:00	-17.3	78.012
14:20:00	-17.3	78.012
14:30:00	-17.3	78.012
14:40:00	-17.3	78.012
14:50:00	-17.3	129.34
15:00:00	-17.3	129.34
15:10:00	-17.3	129.34
15:20:00	-17.3	129.34
15:30:00	-17.3	129.34
15:40:00	-17.3	129.34
15:50:00	-17.3	129.34
16:00:00	-17.3	129.34
16:10:00	-17.3	129.34
16:20:00	-17.3	129.34
16:30:00	-17.3	129.34
16:40:00	-17.3	129.34
16:50:00	-17.3	129.34
17:00:00	-17.3	129.34

References

ASHRAE, 2019. ASHRAE Handbook - HVAC Applications. ASHRAE Inc., Atlanta, US.

Baakeem, S.S., Orfi, J., Alabdulkarem, A., 2018. Optimization of a multistage vapor-compression refrigeration system for various refrigerants. Appl. Therm. Eng. 136, 84–96. <https://doi.org/10.1016/j.applthermaleng.2018.02.071>.

Berhad, T.N., 2014. Electricity Tariff Schedule.

Charef, R., 2022. The use of Building Information Modelling in the circular economy context: several models and a new dimension of BIM (8D). Clean Eng Technol 7, 100414. <https://doi.org/10.1016/j.clet.2022.100414>.

Chen, Y., Xu, J., Wang, J., Lund, P.D., 2022. Optimization of a weather-based energy system for high cooling and low heating conditions using different types of water-cooled chiller. Energy 252, 124094. <https://doi.org/10.1016/j.energy.2022.124094>.

Deng, K., Sun, Y., Li, S., Lu, Y., Brouwer, J., Mehta, P.G., et al., 2015. Model predictive control of central chiller plant with thermal energy storage via dynamic programming and mixed-integer linear programming. IEEE Trans. Autom. Sci. Eng. 12, 565–579. <https://doi.org/10.1109/TASE.2014.2352280>.

FlyCarpet Inc. Online interactive psychrometric chart. <https://www.flycarpet.net/en/psyonline>, 2023.

Gbadamosi, S.L., Nwulu, N.I., 2021. A comparative analysis of generation and transmission expansion planning models for power loss minimization. Sustain Energy, Grids Networks 26, 100456. <https://doi.org/10.1016/J.SEGAN.2021.100456>.

Hartman, T.B., 2001. All-variable speed centrifugal chiller plants. ASHRAE J. 43, 43–53.

Ho, W.T., Yu, F.W., 2021. Chiller system optimization using k nearest neighbour regression. J. Clean. Prod. 303. <https://doi.org/10.1016/j.jclepro.2021.127050>.

Huang, P., Huang, G., Augenbroe, G., Li, S., 2018. Optimal configuration of multiple-chiller plants under cooling load uncertainty for different climate effects and building types. Energy Build. 158, 684–697. <https://doi.org/10.1016/j.enbuild.2017.10.040>.

Kim, D., Wang, Z., Brugger, J., Blum, D., Wetter, M., Hong, T., et al., 2022. Site demonstration and performance evaluation of MPC for a large chiller plant with TES for renewable energy integration and grid decarbonization. Appl. Energy 321, 119343. <https://doi.org/10.1016/j.apenergy.2022.119343>.

- Kong, D., Yin, X., Ding, X., Fang, N., Duan, P., 2021. Global optimization of a vapor compression refrigeration system with a self-adaptive differential evolution algorithm. *Appl. Therm. Eng.* 197, 117427 <https://doi.org/10.1016/j.applthermaleng.2021.117427>.
- Kumar, D., Alam, M., Memon, R.A., Bhayo, B.A., 2022. A critical review for formulation and conceptualization of an ideal building envelope and novel sustainability framework for building applications. *Clean Eng Technol* 11, 100555. <https://doi.org/10.1016/j.clet.2022.100555>.
- Liao, Y., Huang, G., Ding, Y., Wu, H., Fan, C., 2017. Robustness analysis and enhancement of chiller sequencing control under uncertainties. *Procedia Eng.* 205, 1878–1885. <https://doi.org/10.1016/j.proeng.2017.10.270>.
- Liu, Z., Tan, H., Luo, D., Yu, G., Li, J., Li, Z., 2017. Optimal chiller sequencing control in an office building considering the variation of chiller maximum cooling capacity. *Energy Build.* 140, 430–442. <https://doi.org/10.1016/j.enbuild.2017.01.082>.
- Lu, Y., Chen, J., Mo, Y., 2019. Optimal operation strategies for a large multi-chiller system based on cooling load forecast. *J. Software Eng. Appl.* 12, 540–561. <https://doi.org/10.4236/jsea.2019.1212033>.
- Merkert, L., Harjunkoski, I., Isaksson, A., Säynevirta, S., Saarela, A., Sand, G., 2015. Scheduling and energy – industrial challenges and opportunities. *Comput. Chem. Eng.* 72, 183–198. <https://doi.org/10.1016/j.compchemeng.2014.05.024>.
- Nagraj, S.M., Kommadath, R., Kotecha, P., Anandalakshmi, R., 2022. Multi-objective optimization of vapor absorption refrigeration system for the minimization of annual operating cost and exergy destruction. *J. Build. Eng.* 49, 103925 <https://doi.org/10.1016/j.jobe.2021.103925>.
- Sadat-mohammadi, M., Asadi, S., Habibnezhad, M., Jebelli, H., 2020. Energy & Buildings Robust Scheduling of Multi-Chiller System with Chilled-Water Storage under Hourly Electricity Pricing, vol. 218. <https://doi.org/10.1016/j.enbuild.2020.110058>.
- Sala-Cardoso, E., Delgado-Prieto, M., Kampouropoulos, K., Romeral, L., 2020. Predictive chiller operation: a data-driven loading and scheduling approach. *Energy Build.* 208. <https://doi.org/10.1016/j.enbuild.2019.109639>.
- Salari, E., Askarzadeh, A., 2015. A new solution for loading optimization of multi-chiller systems by general algebraic modeling system. *Appl. Therm. Eng.* 84, 429–436. <https://doi.org/10.1016/j.applthermaleng.2015.03.057>.
- Shao, Z., Gholamalizadeh, E., Boghosian, A., Askarian, B., Liu, Z., 2019. The chiller's electricity consumption simulation by considering the demand response program in power system. *Appl. Therm. Eng.* 149, 1114–1124. <https://doi.org/10.1016/j.applthermaleng.2018.12.121>.
- Sun, Y., Xue, H., Wang, W., Wu, S., Wu, Y., Hong, Y., et al., 2020. Development of an optimal control method of chilled water temperature for constant-speed air-cooled water chiller air conditioning systems. *Appl. Therm. Eng.* 180, 115802 <https://doi.org/10.1016/j.applthermaleng.2020.115802>.
- Thangavelu, S.R., Myat, A., Khambadkone, A., 2017. Energy optimization methodology of multi-chiller plant in commercial buildings. *Energy* 123, 64–76. <https://doi.org/10.1016/j.energy.2017.01.116>.
- TNB. Pricing & Tariffs, 2023. Commercial tariffs. <https://www.tnb.com.my/commercial-industrial/pricing-tariffs1/>. (Accessed 19 January 2023).
- Velashjerdi Farahani, A., Jokisalo, J., Korhonen, N., Jylhä, K., Kosonen, R., Lestinen, S., 2022. Performance assessment of ventilative and radiant cooling systems in office buildings during extreme weather conditions under a changing climate. *J. Build. Eng.* 57 <https://doi.org/10.1016/j.jobe.2022.104951>.
- Wang, W., Zhou, Q., Pan, C., Cao, F., 2022a. Energy-efficient operation of a complete Chiller-air handling unit system via model predictive control. *Appl. Therm. Eng.* 201, 117809 <https://doi.org/10.1016/j.applthermaleng.2021.117809>.
- Wang, W., Zhou, Q., Pan, C., Cao, F., 2022b. Energy-efficient operation of a complete Chiller-air handling unit system via model predictive control. *Appl. Therm. Eng.* 201, 117809 <https://doi.org/10.1016/j.applthermaleng.2021.117809>.
- Zhang, Q., Grossmann, I.E., 2016. Enterprise-wide optimization for industrial demand side management: fundamentals, advances, and perspectives. *Chem. Eng. Res. Des.* 116, 114–131. <https://doi.org/10.1016/j.cherd.2016.10.006>.
- Zulkafli, N.I., Kopanos, G.M., 2017. Integrated condition-based planning of production and utility systems under uncertainty. *J. Clean. Prod.* 167, 776–805. <https://doi.org/10.1016/j.jclepro.2017.08.152>.
- Zulkafli, N.I., Sukri, M.F., Tahir, M.M., Muhajir, A., Hanak, D.P., 2022. Optimal operation of chillers plant in academic building by using linear programming approach. *Chem Eng Trans* 97, 91–96. <https://doi.org/10.3303/CET2297016>.